Journal of Zhejiang University-SCIENCE C (Computers & Electronics)
ISSN 1869-1951 (Print); ISSN 1869-196X (Online)
www.zju.edu.cn/jzus; www.springerlink.com
E-mail: jzus@zju.edu.cn

Coordination of PSS and TCSC controller using modified particle swarm optimization algorithm to improve power system dynamic performance

Alireza REZAZADEH[1], Mostafa SEDIGHIZADEH[†‡1,2], Ahmad HASANINIA[1]

([1]*Faculty of Electrical and Computer Engineering, Shahid Beheshti University, Tehran 1983963113, Iran*)

([2]*Faculty of Engineering and Technology, Imam Khomeini International University, Ghazvin 34194, Iran*)

[†]E-mail: m_sedighi@sbu.ac.ir

Received Sept. 6, 2009; Revision accepted Jan. 5, 2010; Crosschecked June 9, 2010; Published online July 10, 2010

Abstract: This paper develops a modified optimization procedure for coordination of a power system stabilizer (PSS) and a thyristor controlled series compensator (TCSC) controller to enhance the power system small signal stability. The new approach employs eigenvalue-based and time-domain simulation based objective functions simultaneously to improve the optimization convergence rate. A modified particle swarm optimization (MPSO) algorithm is used as the optimization algorithm. The results of simulations and eigenvalue analysis for a single machine infinite bus (SMIB) system equipped with the proposed PSS and TCSC controllers confirm that the new approach is effective in enhancing the system stability.

Key words: Coordination, Particle swarm optimization (PSO), Power system stabilizer (PSS), Small signal stability, Thyristor controlled series compensator (TCSC) controller

doi:10.1631/jzus.C0910551 **Document code:** A **CLC number:** TM762

1 Introduction

For many years, improvement of power system dynamic performance has been one of the major issues in power system control and operation. Low frequency oscillations in large interconnected power systems are significant dynamic problems that occur due to the lack of sufficient damping in electromechanical modes. The application of a power system stabilizer (PSS) seems a simple and inexpensive technique for damping these oscillations and enhancing the power system dynamics. Through the injection of a supplementary stabilizing signal at a voltage reference input of an automatic voltage regulator (AVR), PSS produces an amount of damping torque and hence increases the stability of the overall system. Nowadays, conventional fixed-structure PSS is used extensively in power systems.

In recent years, flexible alternating current transmission systems (FACTSs) have been developed as a result of advances in power electronics. FACTS devices such as static var compensator (SVC), static compensator (STATCOM), thyristor controlled series compensator (TCSC), and unified power flow controller (UPFC) are employed in power systems for different purposes. Primary applications of FACTS devices are power flow, reactive power, and voltage controls in transmission systems. Besides these primary functions, FACTS devices are utilized to damp power system oscillations (Larsen *et al*., 1995; Wang, 1999; Wang and Xu, 2004).

TCSC is a FACTS device which is capable of damping electromechanical modes, especially inter-area modes. It is connected in series with the transmission line, and its apparent reactance can be con-

‡ Corresponding author

trolled by varying the firing angle. In damping mode, TCSC must be equipped with a controller to generate the oscillation damping signal. This controller is known as a power oscillation damping (POD) controller.

According to Gibbard *et al*. (2000), uncoordinated local design of PSS and POD controllers in a power system equipped with PSS and FACTS device stabilizers may cause destabilizing interactions. Therefore, coordinated design of PSS and POD controllers will enhance system stability (Pourbeik and Gibbard, 1998; Abido and Abdel-Magid, 2003; Dubey and Dubey, 2006).

Since the coordinated design of power system stabilizers (PSSs and PODs) is a nonlinear problem with a large number of design parameters, it is appropriate to use nonlinear optimization techniques such as the genetic algorithm (GA) and particle swarm optimization (PSO) to solve this problem. GA has already been employed to solve a coordinated design problem in a single machine infinite bus (SMIB) system (Abdel-Magid and Abido, 1999). In addition, Panda and Padhy (2008a) did a comparative study revealing that the convergence rate of PSO is relatively superior to GA for POD controller design.

In this paper, a modified PSO algorithm, known as MPSO, is employed to design the PSS and TCSC controller in an SMIB system simultaneously. Furthermore, a new approach is proposed to enhance the optimization convergence rate.

2 Power system under study

Fig. 1 illustrates the SMIB test system employed for this study. The generator is connected to the infinite bus through the transformer and two transmission lines equipped with the TCSC. X_{L}, X_{T}, and X_{TCSC} represent the reactance of the transmission line, transformer, and TCSC, respectively.

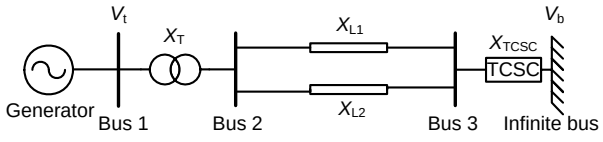

Fig. 1 Single machine infinite bus (SMIB) power system equipped with a thyristor controlled series compensator (TCSC)

The system parameters are given as follows (all data are in p.u. unless specified otherwise).

Generator and excitation system:

$$H = 3.7\ \mathrm{s},\ D = 4.1,\ T'_{\mathrm{d0}} = 4.49\ \mathrm{s},\ x_{\mathrm{d}} = 1.05,\ x_{\mathrm{q}} = 0.474,$$
$$x'_{\mathrm{d}} = 0.296,\ R_{\mathrm{a}} = 0,\ K_{\mathrm{A}} = 100,\ T_{\mathrm{A}} = 0.01\ \mathrm{s},$$

where H is the inertia constant, D the damping coefficient, T'_{d0} the open circuit d-axis transient time constant, x_{d} the d-axis reactance, x_{q} the q-axis reactance, x'_{d} the d-axis transient reactance, R_{a} the armature resistance, K_{A} the gain of the excitation system, and T_{A} the time constant of the excitation system.

Transformer and transmission line:

$$X_{\mathrm{T}} = 0.08,\ X_{\mathrm{L1}} = X_{\mathrm{L2}} = 1,\ X_{\mathrm{TCSC0}} = 0.22,\ V_{\mathrm{b}} = 1,$$

where V_{b} is the infinite bus voltage.

The third-order model comprising the electromechanical swing of the generator and internal voltage equations is used for generator representation. System nonlinear equations can be written as (Kundur, 1994)

$$\dot{\delta} = \omega_0 \cdot \Delta\omega, \tag{1}$$

$$\dot{\omega} = \frac{1}{M}(P_{\mathrm{m}} - P_{\mathrm{e}} - D \cdot \Delta\omega), \tag{2}$$

$$P_{\mathrm{e}} = \frac{E'_{\mathrm{q}} V_{\mathrm{b}}}{X'_{\mathrm{d}}}\sin\delta - \frac{E'_{\mathrm{q}} V_{\mathrm{b}}^2 (x_{\mathrm{q}} - x'_{\mathrm{d}})}{2X'_{\mathrm{d}} X_{\mathrm{q}}}\sin(2\delta), \tag{3}$$

$$\dot{E}'_{\mathrm{q}} = \frac{1}{T'_{\mathrm{d0}}}(-E_{\mathrm{q}} + E_{\mathrm{fd}}), \tag{4}$$

$$E_{\mathrm{q}} = \frac{E'_{\mathrm{q}} X_{\mathrm{d}}}{X'_{\mathrm{d}}} - \frac{V_{\mathrm{b}}(x_{\mathrm{q}} - x'_{\mathrm{d}})}{2X'_{\mathrm{d}} X_{\mathrm{q}}}\cos\delta, \tag{5}$$

$$X_{\mathrm{d}} = x_{\mathrm{d}} + x_{\mathrm{e}},\ X_{\mathrm{q}} = x_{\mathrm{q}} + x_{\mathrm{e}},\ X'_{\mathrm{d}} = x'_{\mathrm{d}} + x_{\mathrm{e}}, \tag{6}$$

where M, δ, and ω are the inertia constant of the synchronous generator, rotor angle, and angular speed of the rotor, respectively. x_{e} is the equivalent reactance between the generator bus and the infinite bus. P_{m} is the mechanical power, and P_{e} is the electrical power. E_{fd} is the excitation voltage, and E_{q} is the internal voltage.

Fig. 2 shows the IEEE TYPE1-ST1 excitation system considered in this study. This model can be

expressed as

$$\dot{E}_{\mathrm{fd}}=\frac{K_{\mathrm{A}}(V_{\mathrm{ref}}-V_{\mathrm{t}}+U_{\mathrm{PSS}})}{T_{\mathrm{A}}}, \tag{7}$$

$$V_{\mathrm{t}}=\sqrt{V_{\mathrm{td}}^2+V_{\mathrm{tq}}^2}, \tag{8}$$

$$V_{\mathrm{td}}=\frac{x_{\mathrm{q}}V_{\mathrm{b}}}{X_{\mathrm{q}}}\sin\delta, \tag{9}$$

$$V_{\mathrm{td}}=\frac{x_{\mathrm{e}}E'_{\mathrm{q}}}{X'_{\mathrm{d}}}-\frac{x'_{\mathrm{d}}V_{\mathrm{b}}}{X'_{\mathrm{d}}}\cos\delta, \tag{10}$$

where V_{ref} and V_{t} are the reference voltage and terminal voltage respectively, and U_{PSS} is the output signal of PSS added to the automatic voltage regulator (AVR) reference input.

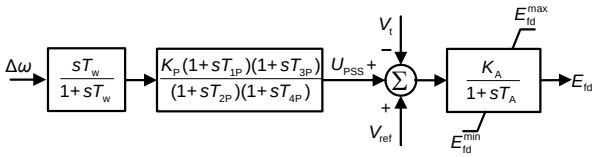

Fig. 2 Block diagram of the excitation system and power system stabilizer (PSS)

In this study a conventional lead-lag controller with a washout filter (to eliminate the DC offset of PSS output) is applied as PSS, and rotor speed deviation is used as feedback signal for PSS.

According to Fig. 3, TCSC consists of a capacitor and an in-parallel-connected thyristor-controlled reactor. The apparent reactance of TCSC varies by changing the thyristor conduction angle (Noroozian *et al*., 1999):

$$X_{\mathrm{TCSC}}(\beta)=K_{\mathrm{B}}(\beta)\cdot X_C, \tag{11}$$

$$K_{\mathrm{B}}=1+\frac{2\lambda^2}{\pi(\lambda^2-1)}\left(\frac{2\cos^2\beta}{\lambda^2-1}\left(\lambda\tan(\lambda\beta)-\tan\beta\right)-\beta-\frac{\sin(2\beta)}{\beta}\right), \tag{12}$$

$$\lambda=\sqrt{X_L/X_C},\ X_C=\omega_0 L,\ X_L=1/(\omega_0 C), \tag{13}$$

where β is the conduction angle, ω_0 is the system angular frequency, and K_{B} is the boost factor of TCSC.

The dynamic behavior of TCSC is considered by time constant T_{TCSC}. TCSC is equipped with a POD controller and uses the generator speed deviation as the feedback signal. A conventional lead-lag controller with a washout filter is used here as a POD controller. Fig. 4 shows how POD control is applied to TCSC, where X_0 is the TCSC steady state reference reactance, which is determined by power flow control.

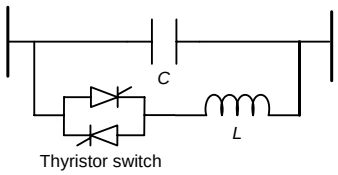

Fig. 3 Thyristor controlled series compensator (TCSC) main circuit components

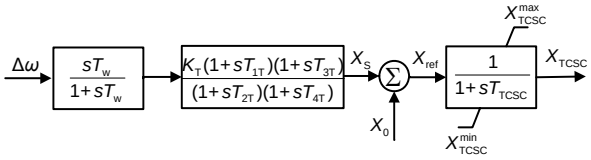

Fig. 4 Block diagram of thyristor controlled series compensator (TCSC) based power oscillation damping (POD) controller

3 Problem formulation

Achieving the maximum possible stability against disturbances is the main goal in the coordinated design procedure, which can be realized by appropriate tuning of PSS and FACTS controllers parameters. According to Figs. 2 and 4, each controller consists of a gain (K), a washout time constant (T_{w}), and four lead-lag block parameters (T_i, i=1, 2, 3, 4). In the present study, the value of 10 s is assigned to T_{w}, which allows low frequency oscillations passing through the controller. Moreover, the time constants T_2 and T_4 are usually pre-specified (Panda *et al*., 2007; Panda and Padhy, 2008b) and in the present study the values of 1 s and 0.5 s are assigned to T_2 and T_4, respectively. The rest of the parameters (i.e., K, T_1, and T_3) will be tuned using the MPSO algorithm to maximize system stability.

The behavior of rotor speed deviation following a disturbance is a suitable criterion for power system stability assessment. Therefore, it can be utilized to construct the time-domain objective function. An appropriate form of time-domain objective function is used here, which is the integral of the time-multiplied absolute value of the speed deviation:

$$J_{\mathrm{t}}=\sum_{x=1}^{N}\int_{t_0}^{t_1} t\left|\Delta\omega(t,x)\right|\mathrm{d}t, \tag{14}$$

where t_0 is the disturbance occurrence time, t_1 is the end of the simulation, and x is the system operating condition. N different operating conditions are considered in the objective function to guarantee the robustness of the stabilizer. The optimization procedure moves toward the solutions with fewer overshoots and less settling time due to the presence of $\Delta\omega$ and t in the objective function, respectively.

Another approach in the power system stability assessment is to utilize a power system linearized model. The power system linearized model is derived by linearization of Eqs. (1)–(10) around an equilibrium point as follows:

$$\begin{cases}\Delta\dot{\delta}=\omega_0\Delta\omega,\\ \Delta\dot{\omega}=\dfrac{1}{M}(-K_1\Delta\delta-K_2\Delta E'_{\mathrm{q}}-K_{\mathrm{P}}\Delta X_{\mathrm{TCSC}}-D\Delta\omega),\\ \Delta\dot{E}'_{\mathrm{q}}=\dfrac{1}{T'_{\mathrm{d0}}}(-K_3\Delta\delta-K_4\Delta E'_{\mathrm{q}}-K_{\mathrm{q}}\Delta X_{\mathrm{TCSC}}+\Delta E_{\mathrm{f}}),\\ \Delta\dot{E}_{\mathrm{f}}=\dfrac{1}{T_{\mathrm{A}}}[-\Delta E_{\mathrm{fd}}-K_{\mathrm{A}}(K_5\Delta\delta+K_6\Delta E'_{\mathrm{q}}+K_{\mathrm{V}}\Delta X_{\mathrm{TCSC}})],\end{cases} \tag{15}$$

where

$$\begin{cases}K_1=\dfrac{\partial P_{\mathrm{e}}}{\partial\delta}, & K_2=\dfrac{\partial P_{\mathrm{e}}}{\partial E'_{\mathrm{q}}}, & K_{\mathrm{P}}=\dfrac{\partial P_{\mathrm{e}}}{\partial X_{\mathrm{TCSC}}},\\ K_3=\dfrac{\partial E_{\mathrm{q}}}{\partial\delta}, & K_4=\dfrac{\partial E_{\mathrm{q}}}{\partial E'_{\mathrm{q}}}, & K_{\mathrm{q}}=\dfrac{\partial E_{\mathrm{q}}}{\partial X_{\mathrm{TCSC}}},\\ K_5=\dfrac{\partial V_{\mathrm{t}}}{\partial\delta}, & K_6=\dfrac{\partial V_{\mathrm{t}}}{\partial E'_{\mathrm{q}}}, & K_{\mathrm{V}}=\dfrac{\partial V_{\mathrm{t}}}{\partial X_{\mathrm{TCSC}}}.\end{cases} \tag{16}$$

Fig. 5 illustrates the block diagram of the linearized SMIB system extended by FACTS devices known as the Philips-Hefferon model. The system eigenvalues can be obtained using eigenvalue analysis. If all of the eigenvalues lie in the left half of the complex plane, the system will be stable. However, the extent of stability depends on the position of eigenvalues in the left-half plane. In the case of the eigenvalues having just real parts, a more negative eigenvalue is an index for a more stable system. But in the case of complex eigenvalues, the damping ratio seems a more suitable criterion for eigenvalue stability measurement. The damping ratio is defined as

$$\xi_i=-\mathrm{Real}(\lambda_i)/|\lambda_i|, \tag{17}$$

where λ_i is the ith eigenvalue.

According to the above explanation, we propose an eigenvalue-based objective function as follows:

$$J_{\mathrm{e}}=\max\{\mathrm{Real}(\lambda_{\mathrm{r}})\}+\max\{k\,|\,\xi_{\mathrm{c}}-\xi^{*}\,|\}, \tag{18}$$

where λ_{r} is the real eigenvalue and ξ_{c} is the complex eigenvalue. The first expression in the objective function reflects the stability of real-valued eigenvalues while the second one reflects the stability of complex eigenvalues. k is a weighting factor balancing the effect of complex eigenvalues with real-valued eigenvalues in the objective function.

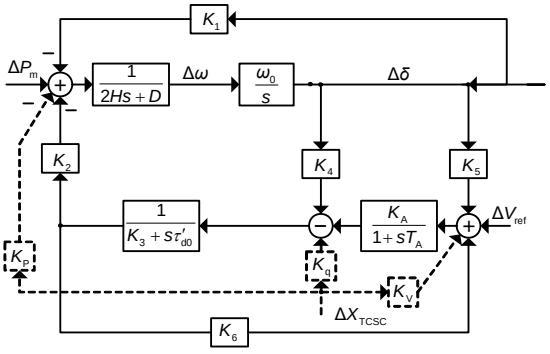

Fig. 5 Philips-Hefferon model extended by the thyristor controlled series compensator (TCSC)

Theoretically, the problem has no constraints. However, due to some practical limitations we must consider a number of constraints. Very large values of the controller gain can result in the operation of the excitation system and TCSC limiters. Hence, an upper limit ($K_{\max}$) must be assigned for the controller gain. Additionally, we can reduce the size of the search space by restricting the lead-lag block parameters. The upper and lower limits are selected with regard to the frequency limits of system modes. These constraints can be written as

$$\boldsymbol{P}_{\min}<\boldsymbol{P}<\boldsymbol{P}_{\max} \tag{19}$$

with

$$\boldsymbol{P}=[K_{\mathrm{T}},K_{\mathrm{P}},T_{1\mathrm{T}},T_{3\mathrm{T}},T_{1\mathrm{P}},T_{3\mathrm{P}}],$$

where subscripts P and T indicate the PSS and TCSC controller parameters, respectively.

4 Overview of particle swarm optimization

Particle swarm optimization (PSO) is a swarm intelligence class method proposed by Kennedy and Eberhart (1995). The PSO is a population-based stochastic optimization algorithm and recently it has acquired wide applications in optimizing design problems because of its simplicity and ability to optimize complex constrained objective functions in multimodal search spaces.

In the PSO each potential solution is referred to as a particle and each set of particles composes a population. Each particle maintains the position associated with the best fitness it ever experiences in a personal memory called pbest. In addition, the position associated with the best value obtained so far by any particle is called gbest. In any iteration, the pbest and gbest values are updated and each particle modifies its velocity to move toward them stochastically. This concept can be formulated as

$$v_i^{t+1}=w\cdot v_i^t+c_1r_1\cdot(\text{pbest}_i-x_i^t)+c_2r_2\cdot(\text{gbest}-x_i^t), \quad (20)$$

$$x_i^{t+1}=x_i^t+v_i^{t+1}, \ i=1, 2, ..., n, \quad (21)$$

where v is the particle velocity, x is the particle position, n is the number of particles, t is the number of iterations, w is the inertia weight factor, c_1 and c_2 are the cognitive and social acceleration factors, respectively, and r_1 and r_2 are the uniformly distributed random numbers in the range (0, 1).

Fig. 6 presents the flow chart of the PSO algorithm for the coordinated design of the PSS and TCSC problem.

Appropriate selection of c_1, c_2, and w plays an important role in effective performance of the PSO. In some cases the convergence is premature, especially for a small inertia weight factor. As the early discovered global best in the searching procedure may be a local minimum, a modified PSO is used to avoid such a case. This variant of PSO has been proposed by Das *et al*. (2006) and is called MPSO. Initially, we define a growth indicator β for each particle, which will be increased if the current fitness value of a particle is smaller than that of the previous iteration. When the personal bests of all particles are updated in each generation, we consider the personal bests having smaller fitness values than the global best as the candidate global best. Finally, the global best will be replaced by the candidate personal best with the highest growth indicator β.

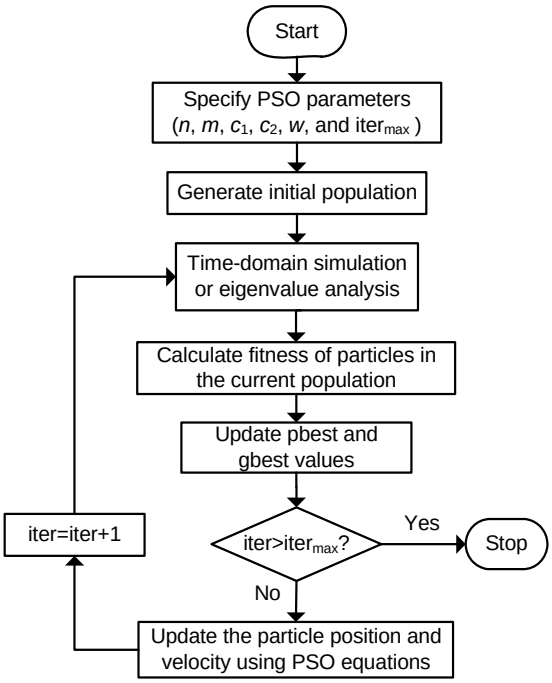

Fig. 6 Flow chart of the particle swarm optimization (PSO) algorithm for coordinated design of the power system stabilizer (PSS) and thyristor controlled series compensator (TCSC) problem

5 The proposed approach

In Section 3, two types of objective function were introduced for the optimized coordinated design of PSS and TCSC. Application of a time-domain objective function leads to a superior solution rather than an eigenvalue-based objective function, since the time-domain objective function employs power system nonlinear equations. However, it will be time consuming to perform nonlinear time-domain simulation any time we need to calculate the fitness value. The eigenvalue-based objective function needs eigenvalues to compute the fitness value, which is evaluated more quickly. But the eigenvalue-based method uses the linearized model of the power system, which in turn decreases the design precision.

It is obvious that the dynamic behavior of the linearized model is approximately similar to that of the nonlinear system around the relevant equilibrium. This means that although the optimum solutions achieved by the two abovementioned objective

functions are not the same, they are close to each other. In this paper, a new optimization approach is proposed to decrease the design procedure time while keeping the design precision. In this method, firstly the optimization is carried out using an eigenvalue-based objective function for a few iterations. This step gives a primary solution. Then, for the next iterations we use the time-domain objective function and the search space is restricted to a small neighborhood of the primary solution. Since the new method reduces the search space, it will improve the convergence time.

6 Simulation and results

To investigate the performance of the proposed approach, the MPSO was performed using MATLAB programming. Initially, we employed the MPSO to optimize eigenvalue-based objective function Eq. (18) in 10 primary iterations. Here the fitness value was evaluated by means of the power system linearized model given by Eqs. (15)–(18). The MPSO parameters and primary optimization results are given in Table 1.

Table 1 Modified particle swarm optimization (MPSO) settings and results for eigenvalue-based optimization

Parameter	Value
MPSO parameters	n=10, c_1=0.6, c_2=0.6, w=1, iter=20
Controller parameters*	
K_P	0, 50, 7.22
T_{1P}	0.1, 3, 0.47
T_{3P}	0.1, 3, 1.77
K_T	0, 70, 49.41
T_{1T}	0.1, 3, 0.37
T_{3T}	0.1, 3, 0.27
Optimization time (s)	1.1

* In each group of controller parameter values, left is the minimum value, middle is the maximum value, and right is the optimized value

Then we used these results to determine the reduced search space as follows:

$$x_0 - \frac{\Delta x}{4} < x < x_0 + \frac{\Delta x}{4}, \tag{22}$$

where x can be K_P, K_T, T_{1T}, T_{3T}, T_{1P}, or T_{3P}, x_0 is the primary solution, and Δx is the initial search space.

Afterward, the time-domain objective function Eq. (14) must be optimized within the reduced search space. In this case the fitness value was determined by performing the time-domain simulation considering a 20% step increase in mechanical power input at t=0.1 s for each set of controller parameters.

To achieve the robust design of stabilizers, three different loading conditions given in Table 2 were considered in the objective function. The MPSO parameters settings were selected by trial and error to have an acceptable convergence rate. The resultant optimal parameters of controllers are given in Table 3. Moreover, the typical convergence of the best fitness value versus the number of iterations is plotted in Fig. 7.

Table 2 Power system loading condition

Loading	Load (p.u.)		
	Low	Nominal	Heavy
P	0.5	0.9	1.20
Q	0.1	0.2	0.25

Table 3 Modified particle swarm optimization (MPSO) settings and results for time-domain optimization in reduced search space

Parameter	Value
MPSO parameters	N=30, c_1=0.25, c_2=0.25, w=0.6, iter=30
Controller parameters*	
K_P	0, 25, 14.34
T_{1P}	0.1, 1.55, 0.43
T_{3P}	0.1, 2.52, 1.31
K_T	11.91, 46.91, 41
T_{1T}	0.1, 1.55, 0.53
T_{3T}	0.1, 1.55, 0.88
Optimization time (s)	10.5

* In each group of controller parameter values, left is the minimum value, middle is the maximum value, and right is the optimized value

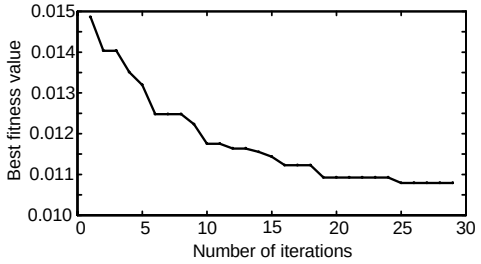

Fig. 7 Best fitness value convergence for time-domain optimization in reduced search space

To compare the proposed method with the conventional optimization method from the viewpoint of the convergence rate, another optimization of Eq. (14) was carried out within the full search space. The related results and convergence of the best fitness value are shown in Table 4 and Fig. 8, respectively.

Table 4 Modified particle swarm optimization (MPSO) settings and results for time-domain optimization in full search space

Parameter	Value
MPSO parameters	n=30, c_1=0.2, c_2=0.2, w=0.6, iter=60
Controller parameters*	
K_P	0, 50, 14.02
T_{1P}	0.1, 3, 0.58
T_{3P}	0.1, 3, 0.86
K_T	0, 70, 42.58
T_{1T}	0.1, 3, 0.51
T_{3T}	0.1, 3, 0.93
Optimization time (s)	19.2

* In each group of controller parameter values, left is the minimum value, middle is the maximum value, and right is the optimized value

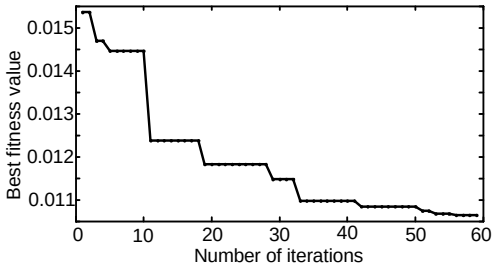

Fig. 8 Best fitness value convergence for time-domain optimization in full search space

A comparison between Figs. 7 and 8 indicates that the convergence rate of the proposed method was considerably superior to that of the conventional method. According to Tables 1, 3, and 4, the total time required in the proposed optimization method was 10.5 s compared to the 19.2 s for the MPSO in full search space. However, both methods approximately led to identical solutions.

Applying eigenvalue analysis to the linearized model of the test system (Fig. 1) is an appropriate means to verify the effect of the proposed stabilizers on small signal stability. Table 5 shows the eigenvalues of the system without any stabilizer, with PSS only and equipped with a coordinated PSS and TCSC controller under nominal loading conditions.

Table 5 Eigenvalues of the test system before and after stabilization

Scheme	Eigenvalues
No control	−63.88, −37.02, −0.065±8.34i
PSS only	−68.33, −28.16, −2.27±8.984i, −1.08, −1.94
Coordinated PSS & TCSC	−69.40, −22.94, −7.49±6.91i, −1.02, −1.98, −2.00, −1.00

In addition, the system dynamic response to the 0.2 p.u. step increase in the mechanical input power of the generator at t=0.5 s was simulated here. The system response to this small disturbance is shown in Figs. 9a–9d. Fig. 9a shows that the system oscillations were undamped without the stabilizer. System oscillations were damped with a settling time of 2.1 s when the PSS was installed on the generator. Furthermore, the simulation results revealed that the system response was well damped with the coordinated PSS and TCSC stabilizer as compared to the PSS only case.

To verify the performance of the proposed coordinated designed stabilizers under severe disturbances, a three-phase fault was simulated. A three-phase fault was applied at bus 2 at t=0.1 s and cleared after 6 cycles by tripping the faulty line. Fig. 10a shows the generator power angle response due to this contingency. The system without control was unstable. In contrast, the system equipped with only PSS was stable even though its overshoot and settling time were not satisfactory. The large disturbance simulation results also indicated that the application of PSS and TCSC controller (in which the controllers were designed by the proposed optimization procedure) led to the best response in view of overshoot and settling time. Therefore, the results verified the effectiveness of the proposed coordinated controllers in enhancing the system stability. Figs. 10b–10d show the variations of $\Delta\omega$, P_e, and ΔV_t under the aforementioned contingency. Note that the permanent tripping of one parallel transmission line for fault clearing increased the transmission line reactance and caused the power angle to increase from 36.4° to 60.2° in the post fault period.

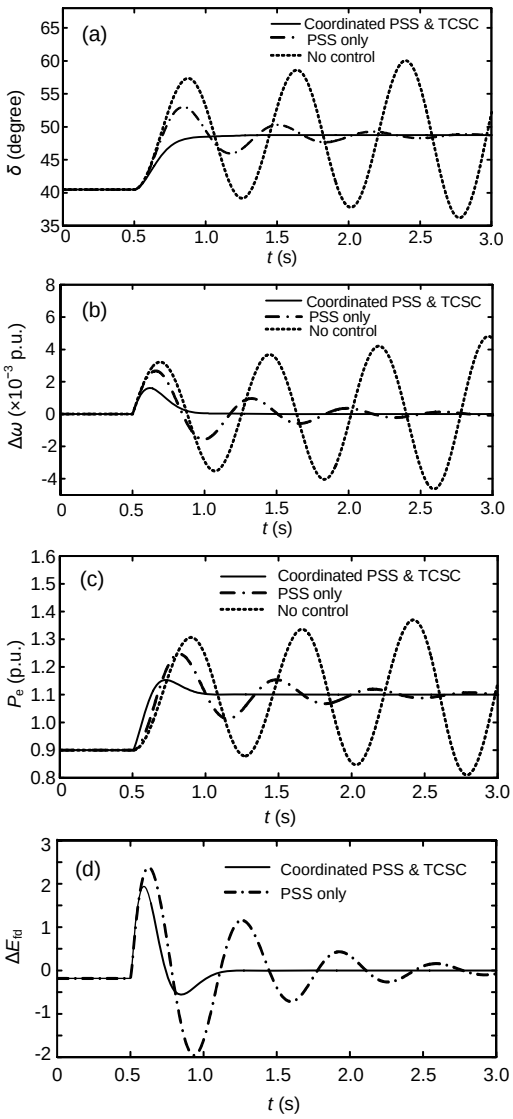

Fig. 9 Power angle (a), $\Delta\omega$ (b), electrical power (c), and ΔE_{fd} (d) variations caused by 0.2 p.u. increase in mechanical power

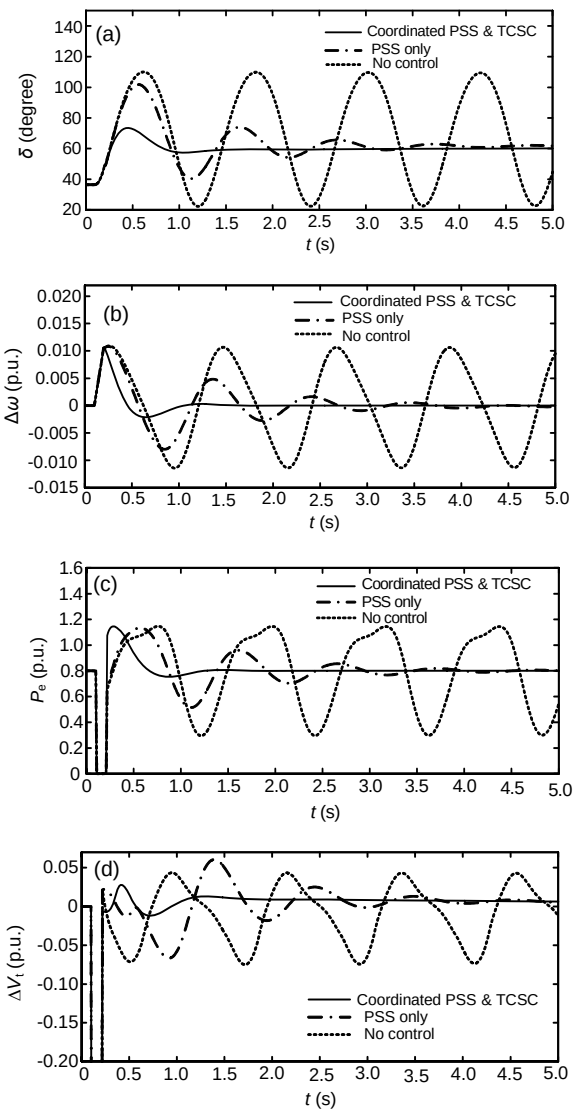

Fig. 10 Power angle (a), $\Delta\omega$ (b), electrical power (c), and ΔV_t (d) response to 6-cycle three-phase fault at bus 2

7 Conclusions

This paper presents an approach for the coordination of PSS and FACTS-based damping controller in an SMIB power system. It uses MPSO as the optimization technique. The new approach employs the eigenvalue- and nonlinear-simulation-based objective functions simultaneously. Optimization results show that the proposed approach decreases the optimization procedure time compared to the conventional method which uses only a nonlinear-simulation-based objective function.

Nonlinear simulation results show the effectiveness of the coordinated PSS and TCSC controller in damping power oscillations. In this study the TCSC is simulated only in the proposed SMIB system; the algorithm is also applicable to other types of FACTS device in multi-machine systems.

References

Abdel-Magid, Y.L., Abido, M.A., 1999. Simultaneous stabilization of multimachine power system via genetic algorithm. *IEEE Trans. Power Syst.*, **14**(4):1428-1439. [doi:10.1109/59.801907]

Abido, M.A., Abdel-Magid, Y.L., 2003. Power System Stability Enhancement via Coordinated Design of a PSS and an SVC-Based Controller. Proc. 10th IEEE Int. Conf. on Electronics, Circuits and Systems, **2**:850-853. [doi:10.1109/ICECS.2003.1301920]

Das, S., Abraham, S., Konar, A., 2006. Spatial Information Based Image Segmentation Using a Modified Particle Swarm Optimization Algorithm. 6th Int. Conf. on Intelligent Systems Design and Applications, **2**:438-444. [doi:10.1109/ISDA.2006.253877]

Dubey, M., Dubey, A., 2006. Simultaneous Stabilization of Multimachine Power System Using Genetic Algorithm Based Power System Stabilizer. Proc. 41st Int. Universities Power Engineering Conf., p.426-431. [doi:10.1109/UPEC.2006.367513]

Gibbard, M.J., Vowles, D.J., Pourbeik, P., 2000. Interaction between, and effectiveness of, power system stabilizers and FACTS device stabilizers in multimachine systems. *IEEE Trans. Power Syst.*, **15**(2):748-755. [doi:10.1109/59.867169]

Kennedy, J., Eberhart, R.C., 1995. Particle Swarm Optimization. Proc. Int. Conf. on Neural Networks, **4**:1942-1948. [doi:10.1109/ICNN.1995.488968]

Kundur, P., 1994. Power System Stability and Control (1st Ed.). McGraw-Hill, New York.

Larsen, E.V., Sanches-Gasca, J.J., Chow, J.H., 1995. Concept for design of FACTS controllers to damp power swings. *IEEE Trans. Power Syst.*, **10**(2):948-956. [doi:10.1109/59.387938]

Noroozian, M., Ängquist, L., Ingeström, G., 1999. Series Compensation in Flexible AC Transmission Systems (FACTS). Institution of Electrical Engineers, London.

Panda, S., Padhy, N.P., 2008a. Comparison of particle swarm optimization and genetic algorithm for FACTS-based controller design. *Appl. Soft Comput.*, **8**(4):1418-1427. [doi:10.1016/j.asoc.2007.10.009]

Panda, S., Padhy, N.P., 2008b. Optimal location and controller design of STATCOM for power system stability improvement using PSO. *J. Franklin Inst.*, **345**(2):166-181. [doi:10.1016/j.jfranklin.2007.08.002]

Panda, S., Padhy, N.P., Patel, R.L., 2007. Robust coordinated design of PSS and TCSC using PSO technique for power system stability enhancement. *J. Electr. Syst.*, **3**:109-123.

Pourbeik, P., Gibbard, M.J., 1998. Simultaneous coordination of power system stabilizers and FACTS device stabilizers in a multimachine power system for enhancing dynamic performance. *IEEE Trans. Power Syst.*, **13**(2):473-479. [doi:10.1109/59.667371]

Wang, H.F., 1999. Oscillation Stability Analysis and Control in Flexible AC Transmission Systems (FACTS). Institution of Electrical Engineers, London.

Wang, H.F., Xu, H.Z., 2004. FACTS-Based Stabilizers to Damp Power System Oscillations: a Survey. 39th Int. Universities Power Engineering Conf., **1**:318-321.

2009 JCR of Thomson Reuters for *JZUS-A* and *JZUS-B*

ISI Web of Knowledge℠

Journal Citation Reports®

WELCOME | HELP | RETURN TO LIST | PREVIOUS JOURNAL | NEXT JOURNAL

2009 JCR Science Edition

Journal: Journal of Zhejiang University-SCIENCE B

Mark	Journal Title	ISSN	Total Cites	Impact Factor	5-Year Impact Factor	Immediacy Index	Citable Items	Cited Half-life	Citing Half-life
☐	J ZHEJIANG UNIV-SC B	1673-1581	619	1.041		0.156	128	3.1	7.5

Journal: Journal of Zhejiang University-SCIENCE A

Mark	Journal Title	ISSN	Total Cites	Impact Factor	5-Year Impact Factor	Immediacy Index	Citable Items	Cited Half-life	Citing Half-life
☐	J ZHEJIANG UNIV-SC A	1673-565X	322	0.301		0.066	213	3.0	6.8

JZUS-A is an international “Applied Physics & Engineering” reviewed-Journal, covering research in Applied Physics, Mechanical and Civil Engineering, Environmental Science and Energy, Materials Science, and Chemical Engineering. *JZUS-B* is an international “Biomedicine & Biotechnology” reviewed-Journal, covering research in Biomedicine, Biochemistry, and Biotechnology. *JZUS-A* and *JZUS-B* were covered by SCI-E in 2007 and 2008, respectively. This is the first time that both journals have gained the Impact Factor.